ELSEVIER

Ceramics International 30 (2004) 817–822

CERAMICS INTERNATIONAL

www.elsevier.com/locate/ceramint

Preparation of MCM-41 with high structural stability

Hyoung-Ho Lee [a], Ji-Whan Ahn [b], Hwan Kim [a,*]

[a] *School of Materials Science and Engineering, Seoul National University, Seoul 151-742, South Korea*
[b] *Institute of Geoscience & Mineral Resources, Taejon 305-350, South Korea*

Received 24 June 2003; received in revised form 22 July 2003; accepted 20 September 2003

Available online 21 March 2004

Abstract

MCM-41 molecular sieves with high structural stability and long-range order were synthesized using ethylamine (EA) as an additive instead of mineralizers such as NaOH and TPAOH. X-ray diffraction showed that the EA/CTAB (cetyltrimethylammonium bromide) ratio was the critical factor that determines the degree of ordering in MCM-41, and an EA/CTAB ratio of 0.2 or 0.5 produced the highest long-range order. The samples had walls approximately 2 nm thick, which is the highest level ever reported. Therefore, they did not lose their structure entirely even after heat treatment at 1000 °C. Together with the effect of the EA/CTAB ratio, the textural mesoporosity, as confirmed from the N_2 adsorption–desorption isotherm analysis, suggests the EA participates in the templating process of the mesostructure.

Keywords: A. Sol–gel processes; B. Porosity; D. Silicate; MCM-41

1. Introduction

Since the discovery of MCM-41 by the scientists from the Mobil Co. at 1992 [1,2], mesoporous molecular sieves (MMS) have aroused a great deal of interest in the area of catalysis due to their potential to overcome the drawback of zeolite—limited diffusion of molecules due to the small channels. Up to now, MMS with pores of sizes ranging from 2 to 30 nm have been developed [3], and are being examined for their catalytic applicability in variable chemical reactions [4,5]. However, the general catalytic processes involve hot water or high temperature conditions, which makes the structure of MMS very weak and unstable due to the hydrolysis of the Si–O–Si bonds and the thin pore walls. Therefore, many studies have focused on improving the structural stability of MMS for catalytic applications [6–8]. The largest reported wall thickness in MCM-41 is 2.68 nm for the sample synthesized hydrothermally at relatively high temperature, 165 °C [9]. In this case, however, partial collapse of porous structure was observed to be inherent, and the structure collapsed for the most part after 1000 °C heat treatment. For the common synthesis conditions, the highest record seems to be around 2 nm [10,11].

It was reported that the structural stability of MMS could be enhanced using small molecule alkylamines as mineralization agents [10]. The authors assumed that the pH buffer function of alkylamines made the building blocks (inorganic precursor) more uniform in terms of the degree of polymerization and the charge density, so leads to a denser channel structure. However, alkylamines with a hydrocarbon chain length of $C > 8$ were reported to act as templates to synthesize MMS with a hexagonal array, which is referred to as HMS [12]. The advantages of HMS materials are a room temperature synthesis process, easy adaptation of foreign atoms other than Si, and thicker walls assuring a high structural stability. Recent reports have shown that even in the case of $C < 8$, alkylamines were utilized as templates to produce microporous materials with a similar mechanism to that of the mesostructure synthesis [13]. Therefore, it is feasible that alkylamines added as mineralization agents have some interactions with the surfactant or inorganic precursor, which have an important effect during the mesostructure forming process.

The aim of this study was to examine the effect of EA existing in the MCM-41 synthesis process to determine its role other than as a mineralization agent, and to

* Corresponding author. Fax: +82-2-884-1413.
E-mail address: hwan94@snu.ac.kr (H. Kim).

0272-8842/$30.00
doi:10.1016/j.ceramint.2003.09.016

synthesize MCM-41 with a high stability as well as a high order.

2. Experimental

2.1. Synthesis of MCM-41

EA was used instead of the common mineralization agents such as NaOH. The reaction mixture had various amounts of CTAB and EA, while with the volumes of TEOS, ethanol and H_2O were fixed. The mixing ratios are shown in Table 1. Initially, solution 1, which was composed of H_2O, CTAB and EA, and solution 2, which was composed of ethanol and TEOS, were mixed for 30 min individually, and then solution 2 was added to solution 1 drop-wise a period of 30 min. The resultant mixture was heated to 80 °C for further 30 min. and maintained at that temperature for 4 h under reflux. The resulting solution was transferred to a Teflon bottle with a

Table 1
Composition of the synthetic mixtures

Sample	Molar composition Si/CTAB/EA/H_2O/EtOH
1CTAB–0.2EA	1.0:1.0:0.2:100:7
1CTAB–0.5EA	1.0:1.0:0.5:100:7
1CTAB–1EA	1.0:1.0:1.0:100:7
1CTAB–2EA	1.0:1.0:2.0:100:7
0.5CTAB–0.2EA	1.0:0.5:0.2:100:7
0.5CTAB–0.5EA	1.0:0.5:0.5:100:7
0.5CTAB–1EA	1.0:0.5:1.0:100:7
0.5CTAB–2EA	1.0:0.5:2.0:100:7
0.2CTAB–0.2EA	1.0:0.2:0.2:100:7
0.2CTAB–0.5EA	1.0:0.2:0.5:100:7
0.2CTAB–1EA	1.0:0.2:1.0:100:7
0.2CTAB–2EA	1.0:0.2:2.0:100:7
0.1CTAB–0.2EA	1.0:0.1:0.2:100:7
0.1CTAB–0.5EA	1.0:0.1:0.5:100:7
0.1CTAB–1EA	1.0:0.1:1.0:100:7
0.1CTAB–2EA	1.0:0.1:2.0:100:7

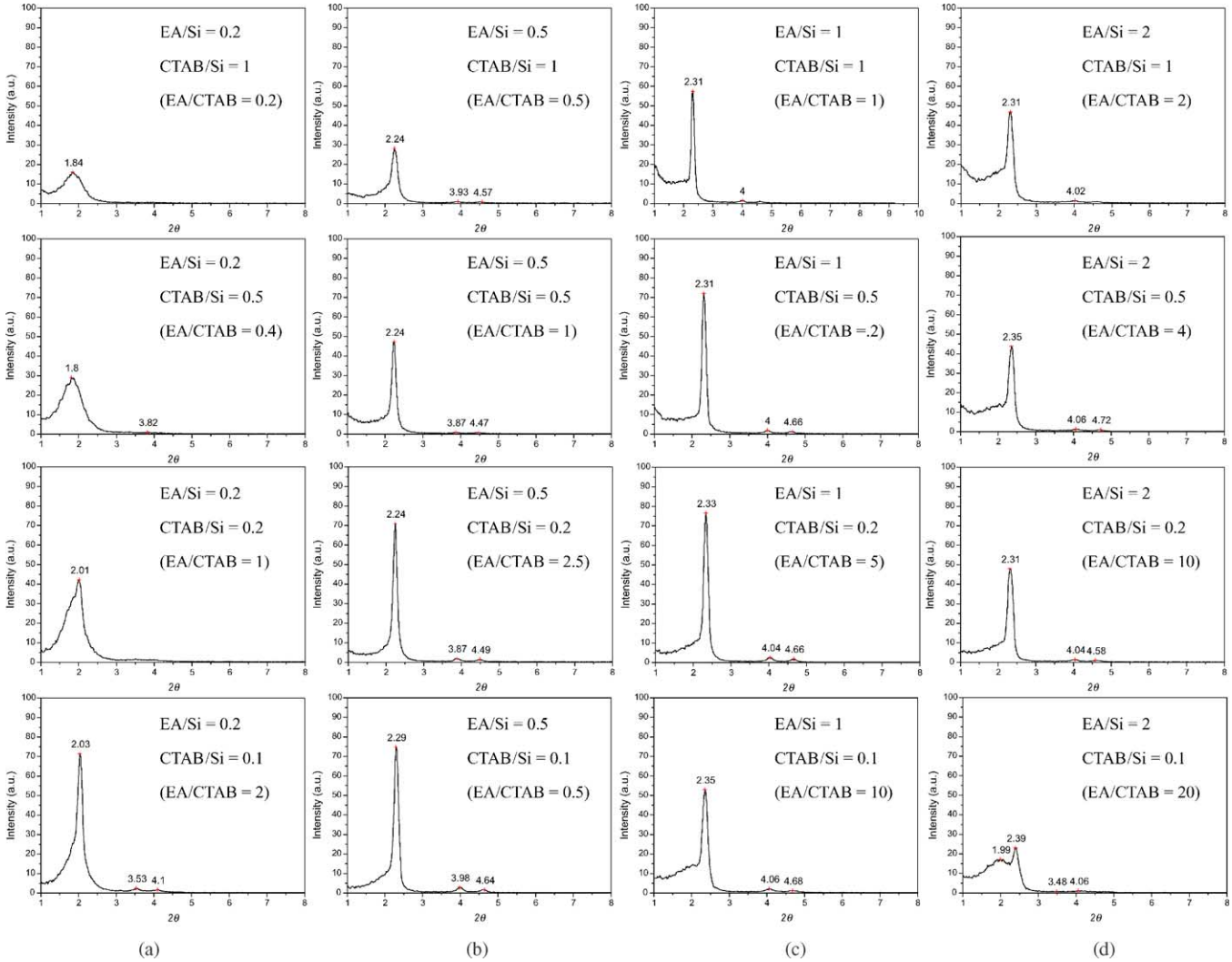

Fig. 1. The SAXS patterns of the products obtained from the initial mixtures with the various EA/CTAB ratios. The EA/Si ratios are (a) 0.2, (b) 0.5, (c) 1 and (d) 2.

sealing cap and left in an oil bath at 100 °C for 3 days. The product was filtered and washed twice with plenty of water, dried in oven at 80 °C overnight, and calcined at 550 °C for 6 h to remove the remaining surfactant.

2.2. Characterization

The microstructure images of the product were obtained using high resolution TEM (Jeol JEM-3000F) operated at an acceleration voltage of 300 kV. Small-angle X-ray scattering (SAXS) data were collected on a Bruker GADDS diffraction system at 40 kV and 30 mA with Cu K_α radiations (λ = 1.5418 Å). The N_2 adsorption–desorption isotherms were obtained using Micromeritics ASAP 2010 for the structural analysis. The specific surface areas were calculated by using the BET method [14], the pore size distributions (PSD) were determined by the BJH method [15]. The structural stability was established using SAXS patterns of heat-treated samples and as-synthesized ones. The wall thickness, which is closely related to the structural stability, was calculated using the lattice parameters obtained from the SAXS patterns and the pore sizes obtained from PSD [11].

3. Results and discussion

The SAXS patterns of the synthesized products are shown in Fig. 1. In the case of EA = 0.2 in Fig. 1(a), a transition from a random structure into nanostructure with a long-range order is observed with decreasing amounts of CTAB. From Fig. 1, it can be seen that increasing the amount of EA or decreasing the amount of CTAB promotes the long-range order of the nanostructure. This tendency can be interpreted in another way in that the intensity of the peaks is strongly affected by the EA/CTAB ratio, and accentuates toward the region of EA/CTAB = 2 or 5. The fact that a similar EA/CTAB ratio gives a similar peak intensity, suggests that the EA affects the template activity of CTAB. Another noteworthy fact shown in Fig. 1 is that when the EA concentration exceeds a certain value, the intensity of the peaks begins to diminish and the amount of CTAB has no effect.

Together with the SAXS patterns, the HRTEM image of one of the synthesized samples shown in Fig. 2 shows the hexagonal arrangement of the MCM-41 mesostructure. Pore-to-pore distance was measured to be approximately 4.3–4.5 nm, which concurs with the result from the SAXS patterns.

Fig. 3 shows the N_2 adsorption–desorption isotherms of the synthesized samples. More prominent jumps in the isotherms can be seen in the high order samples. This coincidence can be also found in a comparison of the SAXS patterns with the pore size distribution curves shown in Fig. 4. The position of the inflection point, which represents the size of the pores, moves toward lower a N_2 partial

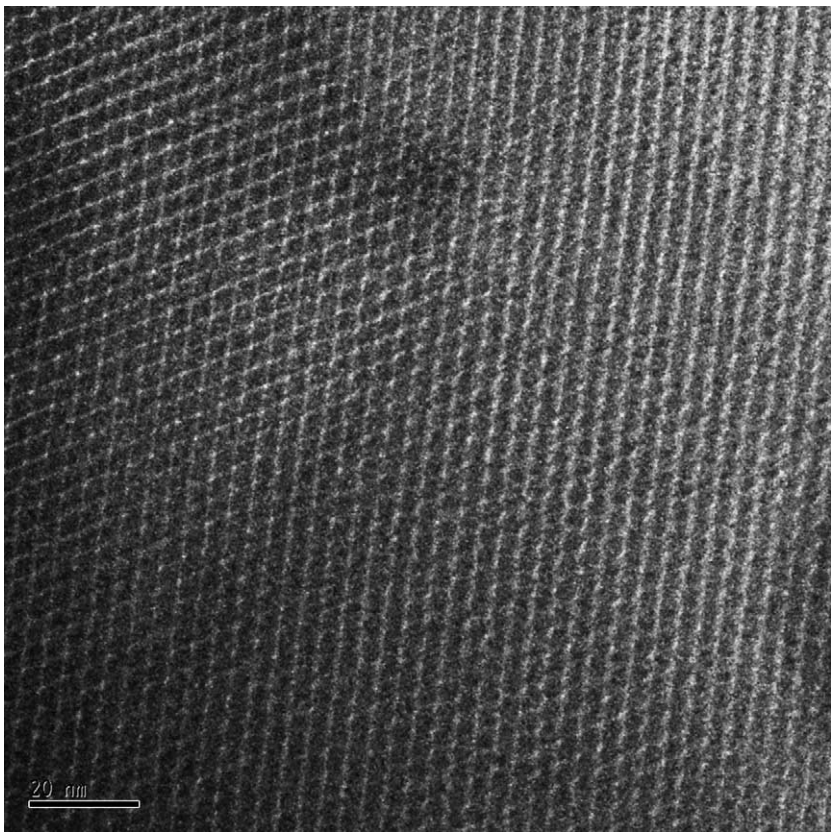

Fig. 2. HRTEM image of a typical sample obtained from an initial mixture of 1Si–0.5EA–0.1CTAB.

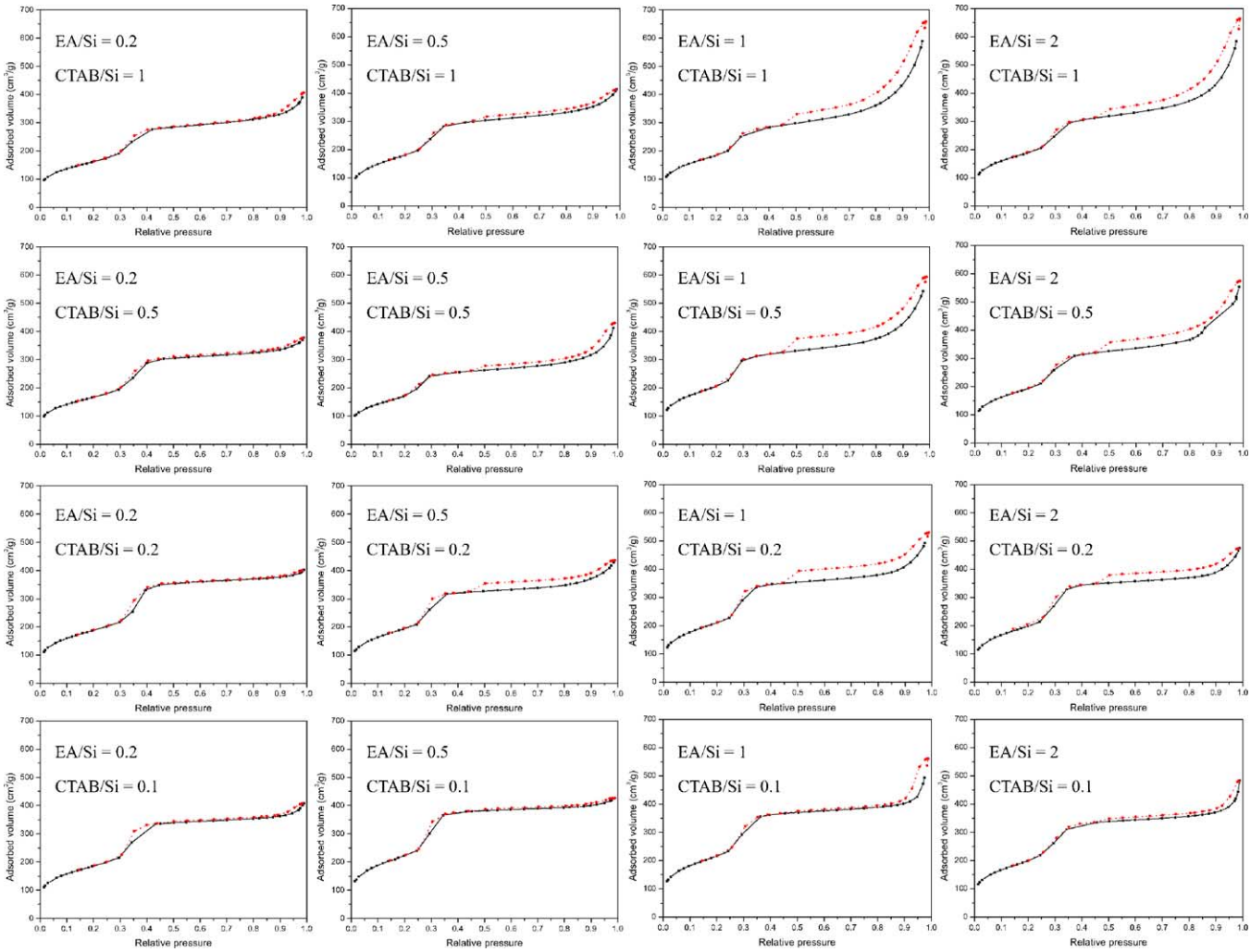

Fig. 3. The N_2 adsorption–desorption isotherms of the products obtained from the initial mixtures with the various EA/CTAB ratios. The desorption branches are shown as dotted lines.

pressure region with increasing EA concentration. However, an increase in the EA concentration also produces a hysteresis loop in the high partial pressure region of the adsorption–desorption isotherm. The results show a bimodal pore size distributions and an increase in the BJH average pore size, although the actual channel sizes decrease. This hysteresis in the high partial pressure region indicates the textural mesoporosity (porosity arising from the spaces formed by interparticle contacts), which is usually observed in HMS materials synthesized by using alkylamines with a hydrocarbon chain length of $C > 8$ as templates [12]. This is another clue indicating that alkylamines play a partial role as a template.

The BET specific surface area and the wall thickness are presented in Table 2. They are in inverse proportion mutually, because the specific surface area means the surface area per gram of samples. Although the wall thickness reduces slightly with better ordering, the wall thickness was

Table 2
Wall thickness and BET surface area of the synthesized samples

1Si–*x*EA–*y*CTAB–100H_2O–7EtOH				
	$x = 0.2$	$x = 0.5$	$x = 1$	$x = 2$
$y = 1$	2.71[a] (580.41)[b]	2.03 (605.29)	1.96 (657.78)	2.03 (680.80)
$y = 0.5$	2.86 (597.70)	2.12 (608.56)	1.93 (735.43)	1.88 (692.77)
$y = 0.2$	2.27 (675.56)	2.05 (696.03)	1.89 (756.29)	1.96 (712.32)
$y = 0.1$	2.21 (666.61)	1.90 (797.56)	1.79 (775.43)	1.71 (714.24)

[a] Wall thickness (nm) = the lattice parameter from the SAXS data—the first maxima in the BJH pore size distribution.
[b] BET surface area (m^2/g).

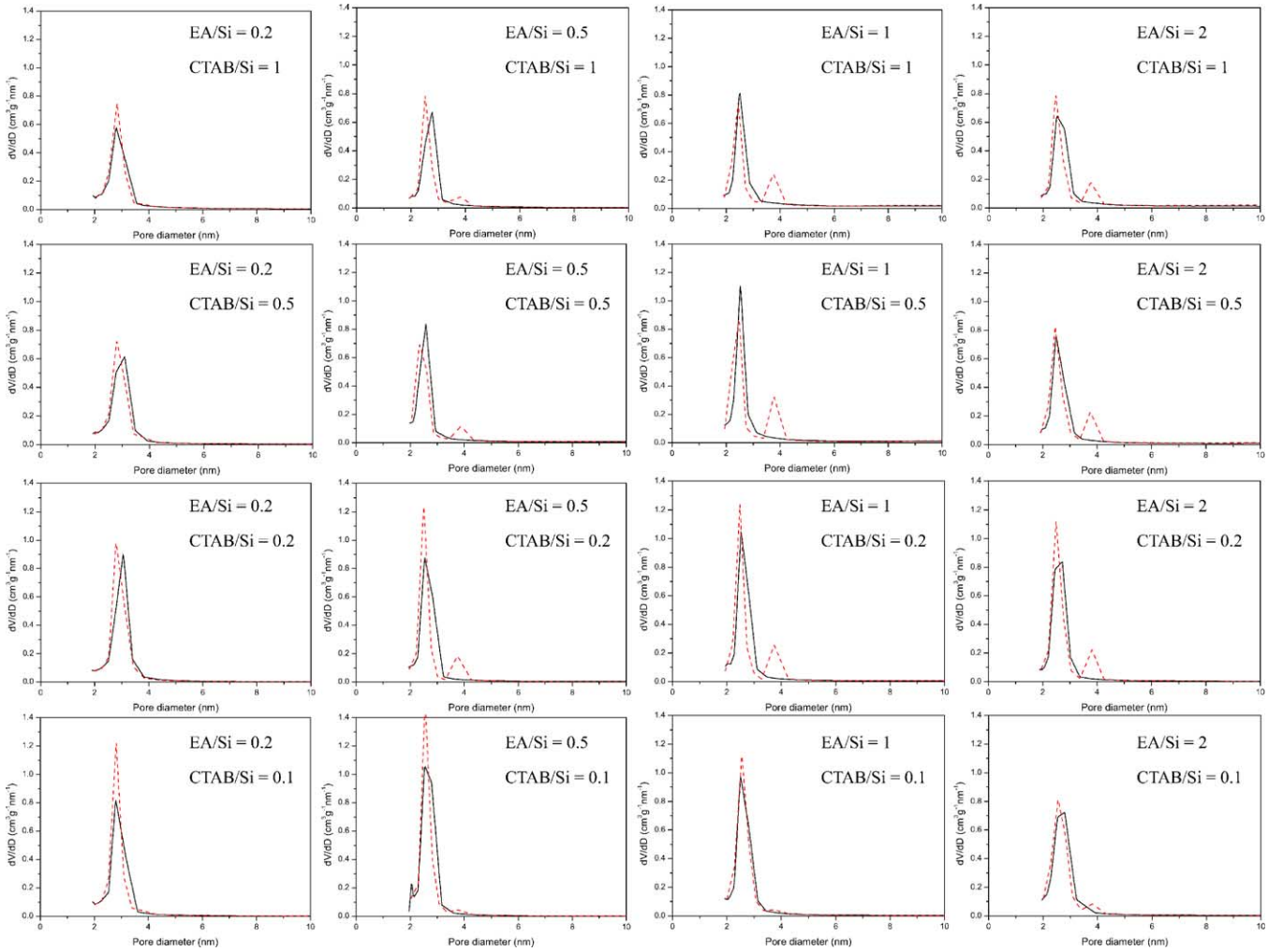

Fig. 4. The BJH pore size distribution curves of the products obtained from the initial mixtures with the various EA/CTAB ratios. The dotted lines are from the desorption branches.

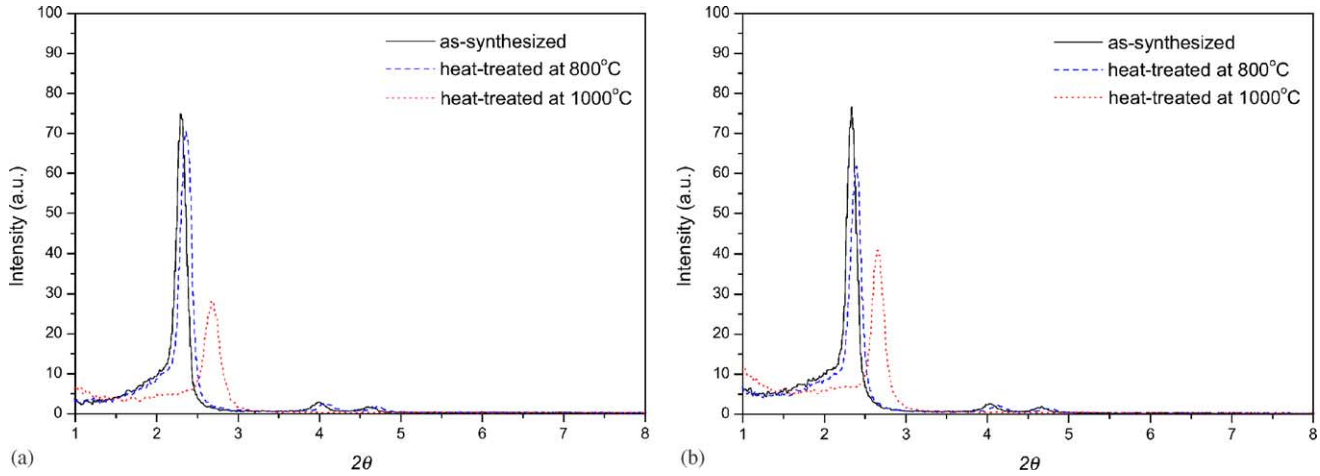

Fig. 5. The SAXS patterns of as-synthesized samples and the heat-treated ones: (a) samples obtained from an initial mixture of 1Si–0.5EA–0.1CTAB, and (b) from 1Si–1EA–0.2CTAB.

approximately 2 nm for all samples, which is the highest level ever reported, promising a high structural stability.

The structural stability was inspected by comparing the SAXS patterns of the samples calcined at 800 or 1000 °C with those of the as-synthesized ones (Fig. 5). The samples calcined at 800 °C maintain their structure. Moreover, the SAXS patterns of those treated even at 1000 °C have about half of the peak intensity. The degree of collapse after heat treatment at 1000 °C is lower in the samples with textural mesoporosity, as Fig. 5 shows. In this case, the complicated textural structure is expected to prohibit the breakdown caused by thermal attack to a certain degree.

4. Conclusions

MCM-41 with both a high stability and a high order was successfully synthesized by adopting the appropriate amount of EA in the TEOS, CTAB and EA system. By using EA instead of the commonly used mineralization agents, the wall thickness of as high as 2 nm could be obtained. The EA/CTAB ratio was found to be the key factor determining the degree of long-range order of the mesostructure. In particular, the highest long-range order was found around the region of EA/CTAB = ~2–5. Together with the influence of the EA/CTAB ratio, the fact that the textural mesoporosity increases with the increasing EA concentration, which is usually observed in HMS materials, suggests that EA plays an important role in the mesostructure-forming process.

Acknowledgements

This research was supported by the 21st century Frontier R & D Project sponsored by the Korea Ministry of Science & Technology.

References

[1] C.T. Kresge, M.E. Leonowicz, W.J. Roth, J.C. Vartuli, J.S. Beck, Nature 359 (1992) 710.
[2] J.S. Beck, J.C. Vartuli, W.J. Roth, M.E. Leonowicz, C.T. Kresge, K.D. Schmitt, C.T.-W. Chu, D.H. Olson, E.W. Sheppard, S.B. McCullen, J.B. Higgins, J.L. Schlenker, J. Am. Chem. Soc. 114 (1992) 10834.
[3] D. Zhao, J. Feng, Q. Huo, N. Melosh, G.H. Fredrickson, B.F. Chmeika, G.D. Stucky, Science 279 (1998) 548.
[4] D. Trong On, D. Desplantier-Giscard, C. Danumah, S. Kaliaguine, Appl. Catal. A: Gen. 253 (2003) 545.
[5] E.P. Barrett, L.G. Joyner, P.P. Halenda, J. Am. Chem. Soc. 73 (1951) 373.
[6] R. Ryoo, S. Jun, J. Phys. Chem. B 101 (1997) 317.
[7] R. Makaya, Angew. Chem. Int. Ed. 38 (19) (1999) 2930.
[8] Do Trong On, Serge Kaliaquine, Angew. Chem. Int. Ed. 41 (6) (2002) 1036.
[9] C.-F. Cheng, W. Zhou, D.H. Park, J. Klinowski, M. Hargreaves, L.F. Gladden, J. Chem. Soc. Faraday Trans. 93 (2) (1997) 359.
[10] W. Lin, Q. Cai, W. Pang, Y. Yue, B. Zou, Microporous Mesoporous Mater. 33 (1999) 187.
[11] H. Chen, Y. Wang, Ceram. Int. 28 (2002) 541.
[12] P.T. Tanev, T.J. Pinnavaia, Chem. Mater. 8 (1996) 2068.
[13] T. Sun, J.Y. Ying, Nature 389 (1997) 704.
[14] S. Brunnauer, P.H. Emmet, E. Teller, J. Am. Chem. Soc. 60 (1938) 309.
[15] E.P. Barrett, L.G. Joyner, P.P. Halenda, Vol. Area Distribut. Porous Substances 73 (1951) 371.